Transcription reinitiation by recycling RNA polymerase that diffuses on DNA after releasing terminated RNA

Wooyoung Kang[1,6], Kook Sun Ha[2,4,6], Heesoo Uhm[1,5], Kyuhyong Park[1], Ja Yil Lee[3], Sungchul Hohng[1]*, Changwon Kang[2]*

[1] Department of Physics and Astronomy, and Institute of Applied Physics, Seoul National University, Seoul 08826, Korea
[2] Department of Biological Sciences, Korea Advanced Institute of Science and Technology, Daejeon 34141, Korea
[3] School of Life Sciences, Ulsan National Institute of Science and Technology, Ulsan 44919, Korea
[4] Present address: Department of Life Science, University of Suwon, Gyeonggi-do 18323, Korea
[5] Present address: Department of Physics, University of Oxford, Clarendon Laboratory, Parks Road, Oxford OX1 3PU, United Kingdom
[6] These authors contributed equally
*Correspondence: ckang@kaist.ac.kr (C.K.); shohng@snu.ac.kr (S.H.)

ABSTRACT

Despite extensive studies on transcription mechanisms, it is unknown how termination complexes are disassembled, especially in what order the components dissociate. Our single-molecule fluorescence study unveils that RNA transcript release precedes RNA polymerase (RNAP) dissociation from DNA template in bacterial intrinsic termination of transcription much more often than concurrent dissociation. As termination is defined by release of product RNA from transcription complex, the subsequent retention of RNAP on DNA constitutes a previously unidentified stage, termed here as 'recycling.' During the recycling stage, RNAPs one-dimensionally diffuse on DNA in downward and upward directions, and these RNAPs can initiate transcription again at nearby promoters in case of retaining a sigma factor. The efficiency of this event, termed here as 'reinitiation,' increases with supplement of a sigma factor. In summary, after releasing RNA product at intrinsic termination, recycling RNAP diffuses on DNA template for reinitiation most times.

INTRODUCTION

Gene expression is regulated at not only initiation but also elongation and termination stages of transcription process for RNA biosynthesis, among other subsequent processes such as RNA processing and transport, and protein synthesis, processing, and targeting. Transcription is terminated with particular RNA sequences that are encoded by terminators in DNA template to effect particular pause of RNA polymerase (RNAP) and eventual disassembly of transcription complexes to release RNA product.

For example, in *Escherichia coli* transcription, RNA structures with a GC-rich hairpin followed by a U-rich tract cause intrinsic (factor-independent) termination, which occurs without any factors although its termination efficiency can be affected by some factors. The U-rich tract makes elongation complex pause to allow for GC-rich RNA hairpin formation that effects conformation changes to destabilize the complex.

Although the structural changes have not been characterized yet, all termination models (Gusarov, I. and Nudler, E., 1999; Ray-Soni A. et al., 2017) include a structural change where DNA·RNA hybrid becomes unstable, which allows RNA to get locally separated from DNA and form hairpins. Single-molecule experiments using optical tweezers have shown that termination mechanisms such as hypertranslocation and shearing mechanisms are terminator-specific (Larson et al., 2008).

However, it is still unknown yet how the complex is broken apart. Especially, which of the three components departs the transcription complex first, RNAP enzyme, RNA product, DNA template, or all together at once? To examine the temporal order of their dissociations and their post-terminational fates in *E. coli* intrinsic termination, we primarily used single-molecule fluorescence measurements.

RESULTS

Construction of Fluorescent Transcription Complex

A primary DNA template (Figure 1A) was synthesized to consist of a 50-bp upstream part including the strong promoter A1 of bacteriophage T7, a 38-bp transcription unit with the intrinsic terminator tR2 of phage λ, and a 15-bp downstream part. It was pre-labeled with Cy5 at the 5' end of template strand (downstream end) and additionally with biotin at the 5' end of nontemplate (coding) strand (upstream end).

In an experiment with radioactive UTP, the major termination site (TS) was +38 position relative to the transcription start site +1, and termination efficiency was 39%. This double-labeled template with a TS-downstream length of 15 bp is denoted by L+15. Likewise, other DNA templates are denoted by L+# with TS-downstream base-pair numbers.

A fluorescent transcription complex with Cy3-labeled RNA was prepared by incubating L+15 with Cy3-labeled ApU, ATP, CTP, GTP, and *E. coli* RNAP holoenzyme with σ^{70} for 30 min in a transcription buffer (Figure 1B). Transcription is initiated preferentially with Cy3-ApU, which is incorporated into the +1 and +2 positions of RNA, but stalled at +12 waiting for the missing UTP. The stalled complexes were immobilized on polymer-coated quartz slides using biotin-streptavidin conjugation.

Fluorescent Detection of Termination and Readthrough

The synchronized, immobilized complexes were then subjected to resumption of elongation by adding all four ribonucleotides (NTPs), while fluorescence images of Cy3-RNA and Cy5-DNA in individual complexes were monitored using total internal reflection fluorescence microscopy. The resumed elongation is followed by either readthrough or termination at TS leading to continued or discontinued downstream transcription, respectively. In the fluorescence images (Figure 1C), vanishing of Cy3-RNA images from the Cy5-DNA spots after NTP addition indicates release of RNA from immobilized DNA, which defines termination of transcription.

In readthrough events, the terminator is ignored by RNAP that passes through TS and continues to transcribe its downstream. With readthrough complexes, from which Cy3-RNA signal is not vanished, protein-induced fluorescence enhancement (PIFE) of Cy5 occurs with red laser excitation (Figure 1D), indicating that RNAP reaches the downstream end of DNA and contacts Cy5 there (Hwang et al., 2011). Additionally, fluorescence resonance energy transfer from Cy3 to Cy5 occurs with green laser excitation, indicating that the 5' end (Cy3) of RNA also approaches the downstream end (Cy5) of DNA presumably due to cotranscriptional folding of RNA.

In termination events, the terminator is recognized by RNAP that ends elongation at TS and does not transcribe its downstream. From termination complexes, Cy3-RNA signal vanishes 4.3±0.3 s after NTP addition (Figure 1E). The termination efficiency measured by frequency of this pathway is 34±4%, similar to the above measured using radioactive incorporation. When ITP is used instead of GTP to destabilize terminator hairpin RNA, this pathway is reduced to 10±1%. Furthermore, this pathway is not observed with a terminator-lacking template L+15M.

RNAP Remaining on DNA After Releasing RNA

Surprisingly, Cy5 PIFE is observed in most (91%) of the termination complexes (Figure 1E). The PIFE starts almost concurrently with Cy3-RNA vanishing and is maintained for 536±82 s (Figure S1), while Cy5 photobleaching takes a much longer time of 2350 s (Figure S2). Accordingly, after termination, most RNAPs keep contacting DNA. This was additionally observed with other intrinsic terminators (Table S3) such as *E. coli his* operon attenuator (87%) and phage ϕ82 t500 terminator (70%), suggesting that the post-terminational retention of RNAP on DNA is general.

To gain further support, we repeated the experiments with Cy5 placed on σ factor rather than DNA (Figure 1F), because the initiation factor has been recently reported to remain in some elongation complexes (Kapanidis et al., 2005; Harden et al., 2016). *E. coli* σ^{70} was labeled with Cy5 at Cys-336 as previously described (Callaci et al., 1998). Cy5-σ is retained in 75% of the initially-stalled complexes (Figure S3), which falls within a previously reported 70-90% range of σ retention (Kapanidis et al., 2005).

This Cy5-σ of holoenzymes mostly (84%) remain on immobilized DNA even after Cy3-RNA vanishing of termination (Figure 1G). In no cases, Cy5-σ vanishes before Cy3-RNA. The dissociation time of σ^{70} (588±85 s, Figure S4) is similar to that of RNAP (536±82 s, Figure S1), suggesting that the holoenzyme maintains a stable complex throughout its retention on DNA.

One-dimensional Diffusion of RNA-free RNAP on DNA

After releasing RNA, RNAP can reach the Cy5-end of DNA through three-dimensional (3D) diffusion after dissociation from DNA or through one-dimensional (1D) diffusion (sliding or hopping) without dissociation from DNA. To examine how RNA-free RNAP reaches DNA ends, a recognition sequence of EcoRI restriction enzyme was inserted into DNA at downstream of TS (Figure 2A). DNA-bound EcoRI blocks procession of *E. coli* RNAP (Epshtein et al., 2003), so this roadblock would obstruct 1D diffusion downward from TS, but not TS-upward 1D diffusion or 3D diffusion.

In experiments using a cleavage-lacking mutant E111Q of EcoRI (Lee et al., 2014), this roadblock reduces PIFE occurrence among the termination complexes when Cy5 is placed at the downstream end of L+112 (from 89±2% to 25±7%), but not with Cy5 placed at the upstream end of L+112R (Figures 2A and 2B). As the PIFE occurrence reduction is as much as DNA cleavage inhibition by E111Q (71±5%; Figure S5), the Cy5-ends are reached by RNAP mostly through 1D diffusion, much more often than 3D diffusion.

Post-terminational Diffusion Lifetime of RNAPs

It is known that RNAP preferentially binds blunt ends of DNA, so the post-terminational retention time of RNAP or σ on short DNA molecules could be longer than the 1D diffusion lifetime, which can be measured on long DNA molecules where diffusing RNAP takes too long to reach an end. The σ-retention time (Cy5 signal duration) after termination was measured on a long DNA of 1560 bp with 6.4% of PIFE occurrence expectation.

The post-terminational diffusion of RNAP lasts for 75±5 s on this long DNA (Figure S6). This lifetime is clearly shorter than RNAP's association with a short DNA of 103 bp at Cy5-end (Cy5-PIFE duration of 536±82 s; Figure S1) or similar association of Cy5-σ holoenzyme with the short DNA (Cy5 signal duration of 588±85 s; Figure S4). RNAP is thus apparently trapped for an extended period once it reaches the ends of DNA.

144

145 **Post-terminational Diffusion Coefficient of RNAPs**

146 The 1D diffusion coefficient of post-terminational RNAPs can be estimated by the correlations
147 that Cy5 PIFE starts later and occurs less frequently as the Cy5-end is placed further away from
148 TS (Figures 2C and 2D). Cy5 PIFE was measured with six templates, L+15, L+62, L+112, L+212,
149 L+312, and L+512, where the distance between TS and Cy5-end of DNA (TS-downstream length)
150 varies from 15 to 512 bp (Figure 2A).

151 Termination efficiency (ranging from 31±3% to 36±16%) or timing (ranging from 4.0±0.8 to
152 7.1±1.3 s) is little affected by the TS-downstream length (Table S1; Figure S7). On the other
153 hand, with increasing TS-end distance, the PIFE start delay increases from 1.8±0.5 to 30±19 s
154 since RNA release (Figure 2C), and the PIFE occurrence decreases from 91% to 47% (Figure 2D),
155 both supporting for 1D diffusion of RNAP on DNA after termination.

156 RNAP diffusion on DNA is modeled to occur with one reflecting end on the surface side and
157 the other absorbing end on the buffer side, which is reasonable because PIFE occurrence at free
158 ends is highly probable with short DNA molecules. This 1D diffusion model adopting the above-
159 determined post-terminational diffusion lifetime of RNAPs fits well to the correlation of the
160 PIFE start timing (R^2 = 0.94) or occurrence (R^2 = 0.96) with the TS-end distance (Figure 2C and
161 2D), from which the diffusion coefficient is estimated as 3.5×10^{-4} or 3.4×10^{-4} $\mu m^2/s$,
162 respectively (see the STAR Methods).

163 On the other hand, the PIFE occurrence data do not fit to a previously described 3D
164 diffusion model (Berg, 1983) (Figure 2D). The PIFE occurrence at zero distance can be
165 additionally estimated by the above 1D diffusion model, and 94% of complexes are estimated
166 to retain RNAP at the time of RNA release at TS, and the remaining 6% release RNAP together
167 with RNA.

168

169 **Transcription Reinitiation by Post-terminational RNAPs**

170 During post-terminational diffusion on DNA, RNA-free holoenzymes of RNAP could initiate
171 transcription again when they encounter a promoter. Even core enzymes of RNAP could do so if
172 they become adequately complemented with σ. Here 'reinitiation' refers to another round of
173 promoter binding and initiation by the RNAP that has released RNA but not fallen off DNA and
174 diffuses on DNA rather than by 3D association of RNAP.

175 Reinitiation was examined using a template with two transcription units (Figure 3A). L+15
176 containing a short transcription unit was extended downstream to contain a roadblock site and
177 another long transcription unit, among other extensions. As explained above, short transcripts
178 from the upstream unit can be labeled with Cy3-ApU, which reports whether termination or
179 readthrough occurs at TS. Long transcripts from the downstream unit contain five repeating 21-
180 bp sequences, and can be probed by a Cy5-labeled DNA oligomer complementary to the repeat

181 sequence.
182 Three courses can proceed (Figure 3B) as they were observed in different types of
183 fluorescence time-traces (Figure 3C). First, reinitiation on the downstream unit occurs after
184 termination from the upstream unit, as Cy5-oligomer probing signal follows Cy3-RNA signal
185 vanishing (type 1). Second, dissociation of RNAP occurs after TS termination, as no Cy5 probing
186 follows Cy3 vanishing (type 2). Third, readthrough occurs for continued downstream
187 transcription, as Cy5 probing follows Cy3 nonvanishing (type 3). The relative frequencies of
188 types 1, 2, and 3 were 0.10±0.05, 0.41±0.10, and 0.49±0.12, respectively.
189 Because transcript probing was not complete, not all readthrough events were counted,
190 and some reinitiation events were observed as type 2 instead of type 1. However, using the
191 measured termination efficiency (34%), the probing efficiency was estimated as 49%, allowing
192 the reinitiation (0.21) and dissociation (0.30) events to be re-sorted (see the STAR Methods).
193 Thus, the reinitiation portion among the termination events was 41% with a mixture of
194 holoenzymes and core enzymes. The reinitiation efficiency decreases to 19% with the above-
195 mentioned roadblock, but increases to 59% with addition of 3 μM σ^{70}.
196
197 **DISCUSSION**
198
199 This study discovered that RNA transcript is released first from transcription complex, and RNAP
200 dissociates from DNA template much later most times in *E. coli* intrinsic termination, based on
201 our single-molecule monitoring of fluorescent RNA transcript, DNA template or σ factor. This
202 sequential release (94%) is much more frequent than their concurrent dissociation (6%).
203 Considering that only 75% of elongation complexes retained σ factor in our case, the post-
204 terminational retention of RNAP on DNA seems to occur similarly with both core and
205 holoenzymes. Additionally, we showed that most holoenzymes retain the σ factor after
206 termination.
207 Because termination should refer to RNA release only, the subsequent retention of RNAP
208 on DNA constitutes a previously unidentified stage. This fourth stage of transcription after the
209 initiation, elongation, and termination stages is here termed as 'recycling' (Figure 4). During the
210 recycling stage, post-terminational RNAPs apparently diffuse on DNA one-dimensionally in
211 downward and upward directions.
212 One-dimensional diffusion of RNAP has been suggested to accelerate promoter search
213 (Singer and Wu, 1987; Ricchetti et al., 1988; Guthold et al., 1999), but few experiments have
214 directly proved it. Furthermore, RNAP diffusion on DNA was recently measured to be too short
215 (<30 ms) to contribute to initiation kinetics under physiological conditions (Wang et al., 2013).
216 This lifetime of pre-initiational RNAP on DNA is much shorter than that of post-terminational
217 RNAP (>1 min) observed in this study, suggesting that their conformations are distinct from

each other. Our single-molecule detection of such long and frequent (95%) retention of post-terminational RNAP on DNA provides the first direct evidence that 1D diffusion of RNAP can dramatically accelerate the promoter search process at least *in vitro*.

RNAP's post-terminational retention of σ and diffusion on DNA allow for transcription reinitiation, which is defined to occur by promoter binding through 1D rather than 3D diffusion of RNAP. Reinitiation is demonstrated here to occur on a downstream promoter oriented in the same direction with the upstream promoter. Although it is not known yet whether 1D-diffusing RNAP can flip to reinitiate at an oppositely oriented promoter, RNAP can diffuse backward or upward towards the upstream end of DNA. Furthermore, σ supplement is shown here to increase the reinitiation efficiency, suggesting that even core enzyme can become reinitiation-competent during the recycling stage, which ends with reinitiation or dissociation of RNAP.

Post-terminational retention and diffusion of RNAP on DNA and transcription reinitiation competence of such RNAP during the recycling stage have several functional implications, although they have not been observed to occur *in vivo* yet. First, they would facilitate transcriptional burst, which has been observed for both bacterial and eukaryotic transcriptions (So et al., 2011; Chong et al., 2014; Fujita et al., 2016). Post-terminational retention of RNAP on DNA during the recycling stage may increase its local density and render it readily convertible into reinitiation-competent state, contributing to the transcriptional burst.

Second, simultaneous transcriptional regulation of multiple operons can be facilitated. In bacterial genomes, functionally related genes and operons are often clustered and regulated together as a regulon (Rocha, 2008; De and Babu, 2010; Meyer and Beslon, 2014; Pannier et al., 2017). One can hypothesize that a single RNAP molecule continually transcribes clustered operons while diffusing on inter-operon regions of DNA chromosome.

Third, transcriptional memory can be facilitated by recycling RNAPs. A loop formed between promoter and terminator is observed in some eukaryotic genes, although not yet in bacterial operons. Such loops can increase initiation efficiency and provide transcriptional memory (Ansari and Hampsey, 2005; Kaderi et al., 2009; Hampsey et al., 2010), where facilitated diffusion of RNAPs on the loop could speed up reactivation.

In this work, we established a single-molecule fluorescence assay to study bacterial transcription termination dynamics. Our construction of fluorescent transcription complexes can permit single-molecule monitoring of their components in studies on transcriptional elongation, termination, recycling, and reinitiation.

ACKNOWLEDGMENTS

We thank Prof. Robert Landick for plasmid pRPODS366C encoding a single-cysteine derivative of σ^{70}. This work was supported by grants from the National Research Foundation of Korea

(2019R1A2C2005209 to SH and 2017R1A2B4002213 to JYL), the High Risk High Return Project of KAIST (N10110078 to CK), and the Research Fund of UNIST (1.160106.01 to JYL).

AUTHOR CONTRIBUTIONS

C.K. and S.H. conceived the study. K.S.H. constructed transcription complexes and performed molecular biology experiments. W.K., H.U., K.P., and J.Y.L. measured the single-molecule fluorescence images and performed biophysics experiments. C.K. supervised the molecular biology part. S.H. supervised the biophysics part. All analyzed the data and contributed to writing of the paper.

DECLARATION OF INTERESTS

The authors declare no competing interests.

FIGURES

Fig. 1. Intrinsic termination observed in single-molecule fluorescence experiments. (**A**) DNA template L+15 with T7A1 promoter and tR2 terminator was pre-labeled with biotin at the upstream end and with Cy5 at the downstream end. RNA transcript was labeled with Cy3 at the 5'-end. (**B**) Experimental scheme. Transcription complexes were stalled, immobilized and then resumed to follow readthrough or termination pathway. (**C**) Cy3-RNA and Cy5-DNA images (black) before and 10 s after NTP addition. Purple circles spot the termination complexes that have lost Cy3-RNA. (**D**-**E**) Representative fluorescence traces at green and red laser excitations from readthrough (D) and termination (E) complexes. Yellow vertical lines indicate NTP addition timing. (**F**) Construct with Cy5 placed on σ^{70} factor. (**G**) Retention of Cy5-σ on DNA after termination (top) more frequent than dissociation (bottom).

282

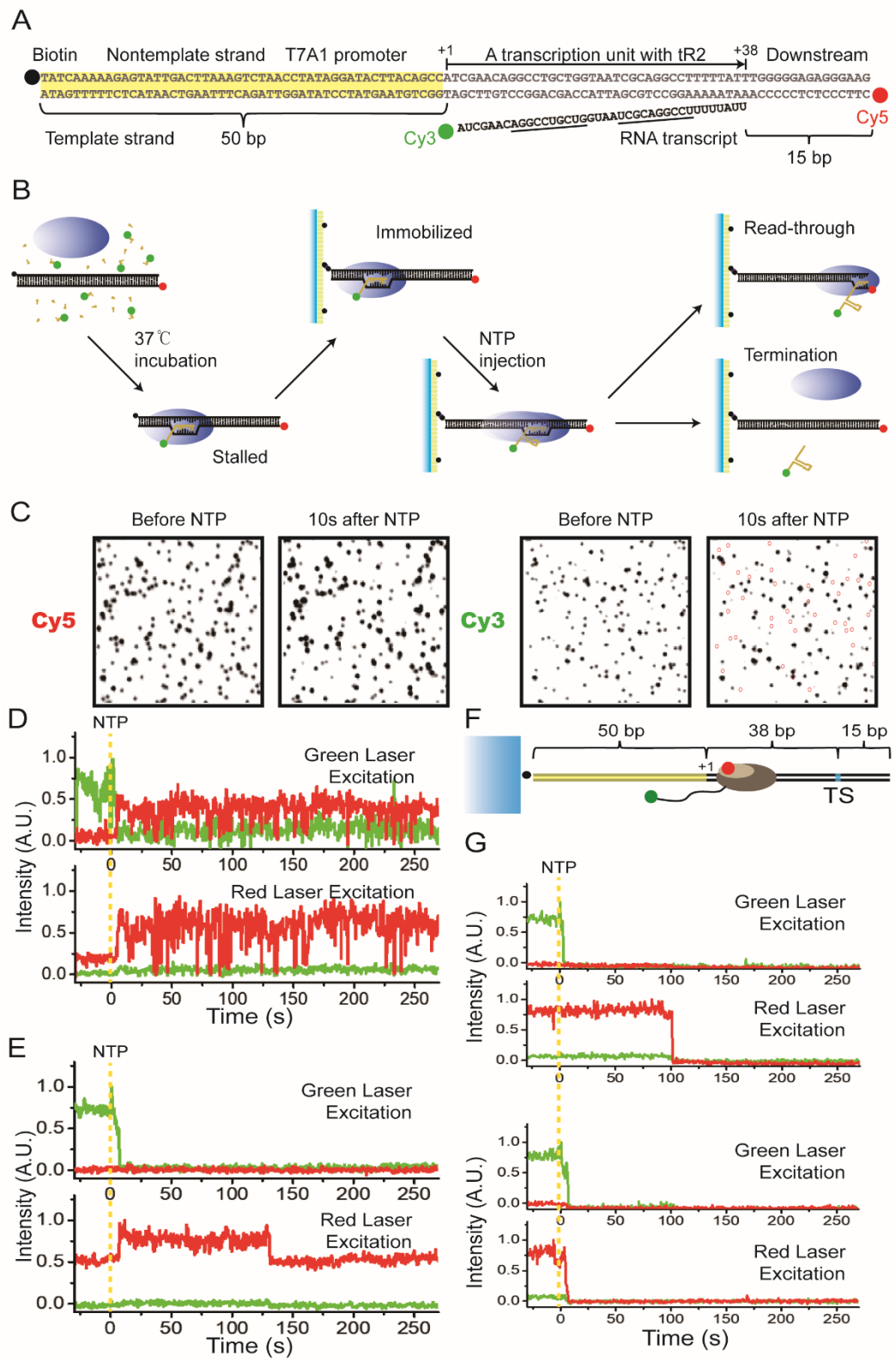
A
Biotin
Nontemplate strand
T7A1 promoter
+1
A transcription unit with tR2
+38
Downstream
TATCAAAAAGAGTATTGACTTAAAGTCTAACCTATAGGATACTTACAGCCATCGAACAGGCCTGCTGGTAATCGCAGGCCTTTTTATTTGGGGGAGAGGGAAG
ATAGTTTTTCTCATAACTGAATTTCAGATTGGATATCCTATGAATGTCGGTAGCTTGTCCGGACGACCATTAGCGTCCGGAAAAATAAACCCCCTCTCCCTTC
Cy5
Template strand
50 bp
Cy3
AUCGAACAGGCCUGCUGGUAAUCGCAGGCCUUUUUAUU
RNA transcript
15 bp
B
Immobilized
Read-through
37℃
incubation
NTP
injection
Termination
Stalled
C
Before NTP
10s after NTP
Before NTP
10s after NTP
Cy5
Cy3
D
NTP
Green Laser
Excitation
Red Laser Excitation
Intensity (A.U.)
Time (s)
E
NTP
Green Laser
Excitation
Red Laser
Excitation
Intensity (A.U.)
Time (s)
F
50 bp
38 bp
15 bp
+1
TS
G
NTP
Green Laser
Excitation
Red Laser
Excitation
Green Laser
Excitation
Red Laser
Excitation
Intensity (A.U.)
Time (s)

283 **Fig. 2. Diffusion of RNAP on DNA after termination.** (**A**) DNA templates with varying distance
284 between TS (cyan) and Cy5-labeled end (red) with or without an EcoRI binding site (purple). (**B**)
285 Reduction of Cy5 PIFE occurrence by a roadblock on L+112 but not L+112R. (**C**) PIFE start
286 timings plotted against TS-end distances. Cy5 PIFE start was timed since Cy3 vanishing from six
287 templates, L+15 through L+512 (black). The timing data fit to a 1D diffusion model (blue). (**D**)
288 PIFE occurrences plotted against TS-end distances. Cy5 PIFE was counted with the six templates
289 (black). The occurrence data fit to the same 1D diffusion model (blue) but not a 3D diffusion
290 model (red).

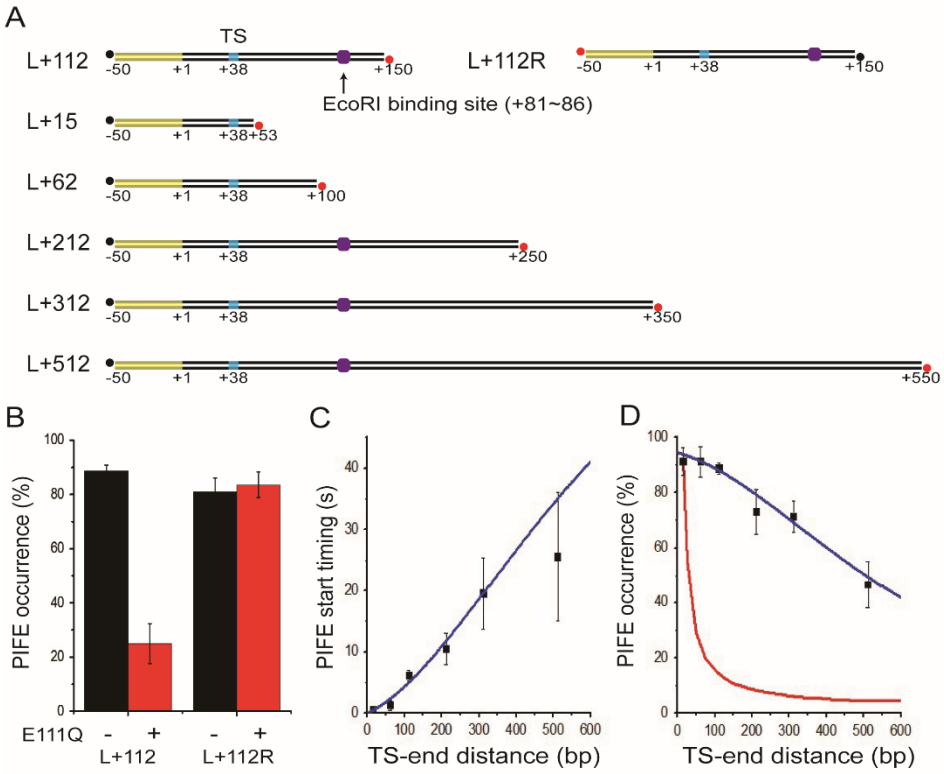

291 **Fig. 3. Detection of transcriptional reinitiation.** (**A**) A DNA template contains two transcription
292 units with a roadblock (purple) between them. Transcripts from the downstream unit have a
293 probing target (brown). (**B**) Three possible courses are reinitiation on the downstream unit after
294 TS termination, dissociation of RNAP after TS termination, and readthrough at TS with
295 continued downstream transcription. (**C**) Three types of fluorescence time-traces were
296 observed; Cy3 vanishing with Cy5 probing (type 1), Cy3 vanishing without Cy5 probing (type 2),
297 and Cy3 nonvanishing with Cy5 probing (type 3).

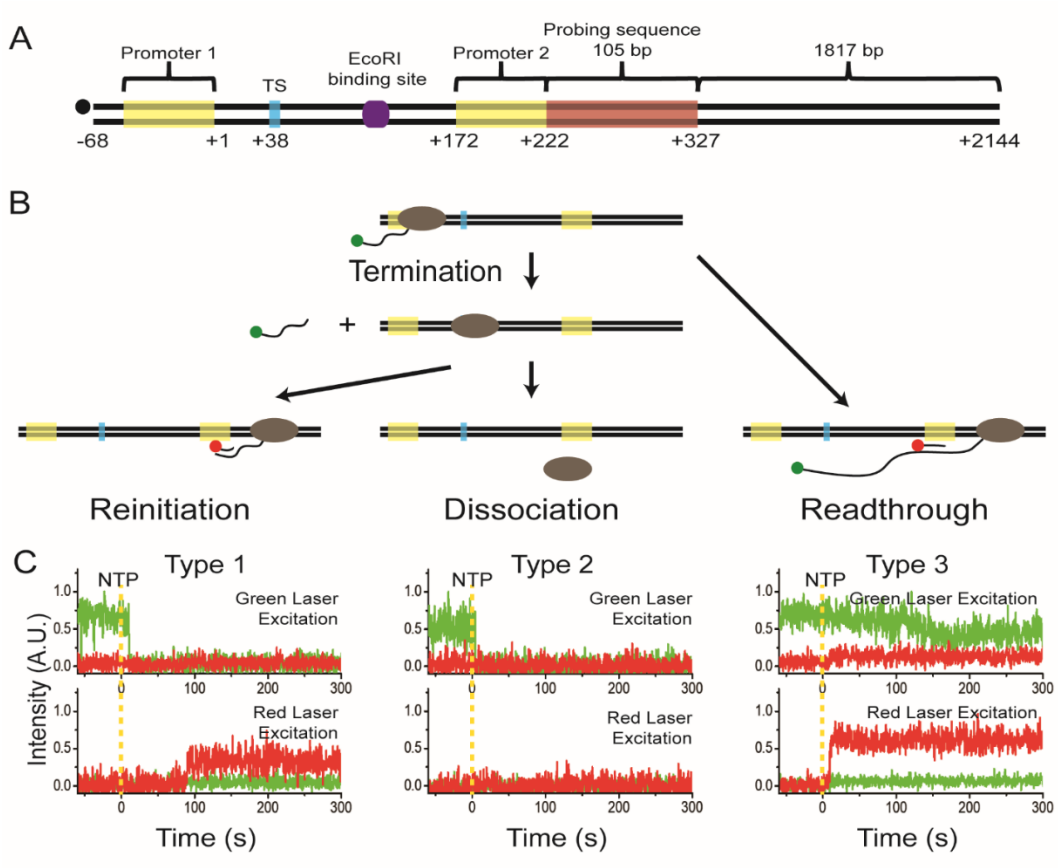

298 **Fig. 4. Four stages of transcription cycle.** (1) Initiation: After binding DNA (black) at a promoter
299 (green), RNAP (cyan) incorporates several NTPs into RNA (blue), and advances downward
300 clearing the promoter. (2) Elongation: RNAP further advances processively downward, resuming
301 from occasional pause or backtrack. (3) Termination: RNAP pauses at a terminator (red) to
302 undergo conformational changes, and releases RNA product. (4) Recycling: RNAP diffuses on
303 DNA downward and upward until it reinitiates transcription at the same or another promoter
304 unless RNAP dissociates off DNA.

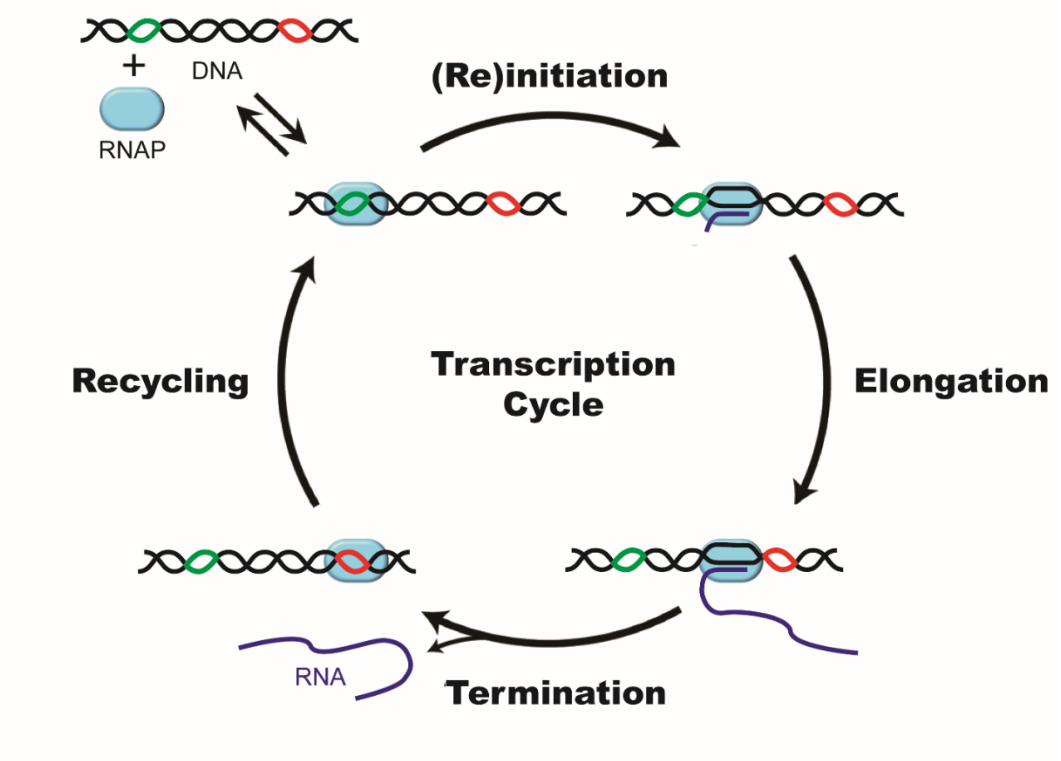

305 **METHODS**
306
307 **Preparation of Transcription Templates**
308 All transcription templates were prepared by polymerase chain reactions using AccuPower
309 ProFi Taq PCR premix from Bioneer, Korea with the amplification templates and primers
310 purchased from Integrated DNA Technologies, USA. Their sequences are listed in table S3. All
311 amplification products were purified using the Cleanup kit Expin PCR SV mini from GeneAll,
312 Korea.
313 DNA template L+15 was prepared using UP8_template, 5' biotin-labeled forward_primer_
314 biotin, and 5' Cy5-labeled reverse_primer_L+15; L+15M using UP8M_template, 5' biotin-labeled
315 forward_primer_biotin, and 5' Cy5-labeled reverse_primer_L+15M; L+62 using UP8_template,
316 5' biotin-labeled forward_primer_biotin, and 5' Cy5-labeled reverse_primer_L+62; L+112 using
317 UP8_template_2, 5' biotin-labeled forward_primer_biotin, and 5' Cy5-labeled reverse_primer_
318 L+112; and L+112R using forward_primer_Cy5' and reverse_primer_biotin instead. Template
319 for phage ϕ82 t500 terminator was prepared using t500_template, 5' biotin-labeled forward_
320 primer_biotin, and 5' Cy5-labeled reverse_primer_L+62; and template for *E. coli his* operon
321 attenuator using his_template, 5' biotin-labeled forward_primer_biotin, and 5' Cy5-labeled
322 reverse_primer_L+62.
323 For L+212 and L+312 constructions, L+112 and additional_part_1 were annealed with
324 DNA_splint_1 by cooling from 90°C to 30°C for 120 min in the annealing buffer (10 mM Tris-HCl,
325 pH 8.0, with 50 mM NaCl), ligated using T4 DNA ligase 2 purchased from New England Biolabs
326 (NEB), USA, and used for amplification reactions. L+212 was prepared using forward_primer_
327 biotin and reverse_ primer_L+212; L+312 using forward_primer_biotin and reverse_primer_
328 L+312. For L+512 construction, L+312 and additional_ part_2 were annealed with DNA_splint_2
329 and the same ligation reaction was repeated. L+512 was prepared using forward_primer_biotin
330 and reverse_primer_L+512.
331 For templates used for reinitiation detection and σ retention time estimation, long_tail
332 template with HindIII recognition sequence was prepared using lambda DNA (NEB),
333 lambda_forward_primer, and lambda_reverse_primer. To construct the upstream part of
334 reinitiation template, L+112_α was prepared with UP8 template_2, forward_primer_extension,
335 and 5' reverse_primer_L+112. L+112_α and reinitiation_part_1B were annealed with
336 DNA_splint_reinitiation by cooling from 90 to 30 °C for 120 min in the annealing buffer, and the
337 same ligation reaction was repeated. Long_tail DNA, the upstream part of reinitiation template,
338 and L+512 were each digested with HindIII (NEB) for one h at 37 °C in the CutSmart™ buffer
339 (NEB). After that, HindIII was deactivated for 20 min at 80 °C.
340 Long_tail DNA were annealed with cleaved L+512 or the upstream part of reinitiation
341 template by the same protocol as above and used for amplification reaction. L+lambda was

342 prepared using forward_primer_biotin and lambda_forward_primer. DNA template for
343 reinitiation detection was prepared using forward_primer_biotin_α and lambda_reverse_
344 primer.
345
346 **Preparation of Cy5-Labeled σ Factor**
347 An N-terminal His_6-tagged *E. coli* σ^{70} was produced in BL21(DE3) cells at 25 °C. Soluble fractions
348 of cell lysates were purified by a 5-ml HisTrap column (GE Healthcare) followed by a 5-ml HiTrap
349 heparin column (GE Healthcare). Purified σ^{70} was incubated with Cy5 maleimide mono-reactive
350 dye (1 mM, GE Healthcare) in the storage buffer (50 mM Tris-HCl, pH 8.0, 100 mM NaCl, and 0.1
351 mM EDTA) overnight at room temperature. Unreacted Cy5-maleimide molecules were removed
352 using an Amicon ultra centrifugal filter (Merck).
353
354 **Single-Molecule Transcription Termination Experiments**
355 To construct a transcription complex, we incubated DNA template (50 nM) with *E. coli* RNAP
356 holoenzyme (20 nM, NEB), ATP, GTP, CTP (20 µM each, GE Healthcare), and Cy3-labeled ApU
357 (250 µM, TriLink) for 30 min at 37 °C. For the experiments with Cy5-labeled σ, we used *E. coli*
358 RNAP core enzyme (20 nM, NEB) plus 1 µM Cy5-σ instead of RNAP holoenzyme. Quartz slides
359 were cleaned using piranha solution to remove organic residues, incubated with (3-
360 aminopropyl)trimethoxysilane (United Chemical Technologies), and coated with polymers by
361 incubating the slides in a 1:40 mixture of biotin-PEG-5000 and m-TEG-5000 (Laysan Bio). The
362 slides were treated with streptavidin (0.2 mg/ml, Invitrogen) for 5 min, and transcription
363 complexes were immobilized on the surface of quartz slides via biotin-streptavidin conjugation.
364
365 **Single-molecule Fluorescence Imaging**
366 A home-made total-internal-reflection fluorescence microscope is equipped with a 532-nm
367 green laser (EXLSR-532-50-CDRH, Spectra-physic) for Cy3 excitation and with a 640-nm red laser
368 (EXLSR-635C-60, Spectra-physic) for Cy5 excitation. An electron multiplying charge-coupled
369 device camera (Ixon DV897, Andor Technology) was used as an imaging device and controlled
370 by using a customized C# program. All experiments were performed at 37 °C with 0.05 s
371 exposure time. The time resolution of the experiments was 0.1 s because we used the
372 alternating laser excitation (ALEX) mode.
373 All experiments were performed with an oxygen scavenging buffer (10 mM Tris-HCl, pH 8.0,
374 20 mM NaCl, 20 mM $MgCl_2$, 1 mM dithiothreitol, 5 mM 3,4-protocatechuic acid, and 100 nM
375 protocatechuate-3,4-dioxygenase) and 200 µM NTP each. In the roadblock experiments, the
376 immobilized transcription complexes were incubated with E111Q (1 nM) for 10 min, and DNA
377 templates without E111Q were digested using wild-type EcoRI (10 units/µl, Beams
378 Biotechnology). Then, we performed the experiments in the oxygen scavenging buffer

containing 1 nM E111Q.

Single-molecule Transcription Reinitiation Experiments

The imaging buffers before and after NTP injection contained the same concentration of Cy5-labeled 'imager DNA' (50 nM, Cy5-TGTGT GTGGT CTGTG GTGTC T) to maintain the same background level. From our analysis were excluded the traces that showed Cy5 signal before NTP addition (nonspecific probing). Because tR2 termination occurs at 4.3 s after NTP addition on average, only Cy3 vanishing within 15 s was regarded as termination. Among these traces, we classified those with Cy5 probing within 240 s as type 1 and the others as type 2. On the other hand, those with Cy3 surviving longer than 180 s and Cy5 probing within 240 s were classified as type 3. Other traces were excluded from data analysis. The exclusion due to Cy3 survival within the range of 15 to 180 s was minor (11%). The exposure time of 0.2 s was used to reduce photobleaching.

QUANTIFICATION AND STATISTICAL ANALYSIS

One-dimensional Diffusion Model

Diffusion of RNAP on DNA can be modeled as 1D diffusion of a point particle with one reflecting end and one absorbing end. RNAP diffusion coefficient and RNAP retention on DNA such as PIFE occurrence and start timing can be estimated using this model.

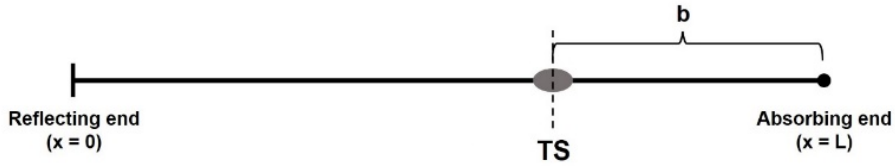

The mean time to reach the absorbing end, $W(x)$, is defined as a function of the distance between the reflecting end and termination site (TS), x. Then, $W(x)$ satisfies the equation (1).

$$W(x) = \tau + \frac{1}{2}[W(x-\delta) + W(x+\delta)] \qquad (1)$$

where δ is a step size of the random walk of the particle moving rightward or leftward every τ s. Because RNAP does not remain on DNA permanently, an RNAP dissociation term is added to the equation (1).

$$W(x) = \tau + \frac{1}{2}(1 - \frac{\tau}{t_{dis}})[W(x-\delta) + W(x+\delta)] \qquad (2)$$

where t_{dis} is a dissociation time of RNAP after termination. In the limit $\delta \to 0$, we can get the differential equation (3) for $W(x)$.

$$W(x) - \mathrm{t}_{dis} = \mathrm{t}_{dis} D \frac{\partial^2}{\partial x^2} W(x) \qquad (3)$$

where D is a diffusion coefficient, defined as $\delta^2/2\tau$.

When TS is positioned at the reflecting end ($x = 0$), the mean capture time does not change with *x*. When TS is positioned at the absorbing end ($x = \mathrm{L}$), the particle is captured right after the particle release, generating the boundary conditions (4) and (5).

$$\frac{dW}{dx}_{x=0} = 0 \quad (4) \qquad \mathrm{W(L)} = 0 \quad (5)$$

With these boundary conditions, the equation (3) is solved as a function of *x* and the total length *L* as shown in equation (6).

$$W(x;L) = t_{dis}\left(1 - {\cosh(x/l_D)}\Big/{\cosh(L/l_D)}\right) \quad (6)$$

where l_D^2 is equal to t_{dis}D. Since *x* is fixed as 88 bp in our experiments, we can rewrite the equation (6) as a function of the distance between TS and the absorbing end, denoted by b.

$$W(b) = t_{dis}\left(1 - {\cosh(88/l_D)}\Big/{\cosh((88+b)/l_D)}\right) \quad (7)$$

Diffusion coefficient of RNAP can be estimated by fitting PIFE timing data to the equation (7).

Similarly, the probability of capture on the absorbing end, *P*(*x*), is defined as a function of x. Then, *P*(*x*) also satisfies the equation (8).

$$P(x) = \frac{1}{2}\left(1 - \frac{\tau}{t_{dis}}\right)[P(x-\delta) + P(x+\delta)] \quad (8)$$

In the limit $\delta \to 0$, we can get the differential equation (9) for *P*(*x*).

$$P(x) = \mathrm{t}_{dis} D \frac{\partial^2}{\partial x^2} P(x) \quad (9)$$

When TS is positioned at the reflecting end, the probability of capture also does not change with x. Otherwise, the probability of capture is equal to the RNAP retention probability during termination at TS when TS is positioned at the absorbing end. These two conditions generate two boundary conditions (10) and (11).

$$\frac{dP}{dx}_{x=0} = 0 \quad (10) \qquad \mathrm{P(L)} = y_0 \quad (11)$$

where y_0 is the RNAP retention probability during termination at TS. With these boundary conditions, we can solve the equation (9) to get the equation (12).

$$P(x;L) = y_0 {\cosh(x/l_D)}\Big/{\cosh(L/l_D)} \quad (12)$$

We can rewrite the *P*(*x*) as a function of b.

$$P(b) = y_0 {\cosh(88/l_D)}\Big/{\cosh((88+b)/l_D)} \quad (13)$$

RNAP retention probability during termination at TS can be estimated by fitting PIFE occurrence to the equation (13).

Calculation of Reinitiation Efficiencies

Among the three types of fluorescence traces of Fig. 3C, type 3 uniquely represents TS-readthrough events (Fig. 3B), but does not cover all of them because transcript probing is not

442 complete. The unprobed readthrough events are not distinguishable from non-activated events
443 and could not be directly counted.
444 On the other hand, types 1 (0.101) and 2 (0.406) together represent total TS-termination
445 events (Fig. 3B), but their sum (0.507) is an overestimation because of incomplete probing.
446 However, using the measured termination efficiency of 33.5%, the unprobed readthrough
447 events (type 4) can be estimated to be 0.513, i.e. (0.507−0.335)/0.335. Types 3 (0.493) and 4
448 (0.513) together represent total readthrough events (1.006), with probing efficiency of 49.0%.
449 Then, total readthrough and termination events become 1.513.
450 Due to incomplete probing, some reinitiation events must have been shown as type 2
451 instead of type 1. Assuming that probing efficiency was the same in readthrough and
452 termination events, total probed and unprobed reinitiation events can be estimated to be 0.206
453 (= 0.101/0.490), and the remaining dissociation events being 0.301 (= 0.507 − 0.206). Thus, the
454 reinitiation portion among the total termination events is 40.6% (= 0.206/0.507) with a mixture
455 of holoenzymes and core enzymes.
456
457 **REFERENCES**
458
459 Ansari, A. & Hampsey, M. (2005). A role for the CRF 3'-end processing machinery in RNAP II-
460 dependent gene looping. Genes Dev. *19*, 2969.
461 Berg, H.C. (1983). Random Walks in Biology (New Jersey: Princeton University Press), pp.37-47.
462 Callaci, S., Heyduk, E. & Heyduk T. (1998). Conformational changes of Escherichia coli RNA
463 polymerase σ^{70} factor induced by binding to the core enzyme. J. Biol. Chem. *273*, 32995-
464 33001.
465 Chong, S., Chen, C., Ge, H. & Xie, X.S. (2014). Mechanism of transcriptional bursting in bacteria.
466 Cell *158*, 314-326.
467 Clerte, C., Declerck, N. & Margeat, E. (2013). Competitive folding of anti-terminator/terminator
468 hairpins monitored by single molecule FRET. Nucleic Acids Res. *41*, 2632-2643.
469 De, S. & Babu, M.M. (2010). Genomic neighborhood and the regulation of gene expression.
470 Curr. Opin. Cell Biol. *22*, 326–333.
471 Epshtein, V., Toulme, F., Rahmouni, A.R., Borukhov, S. & Nudler E. (2003). Transcription through
472 the roadblocks: the role of RNA polymerase cooperation. EMBO J. *22*, 4719-4727.
473 Fujita, K., Iwaki, M. & Yanagida, T. (2016). Transcriptional bursting is intrinsically caused by
474 interplay between RNA polymerases on DNA. Nat. Commun. *7*, 13788.
475 Gusarov, I. & Nudler, E. (1999). The mechanism of intrinsic transcription termination. Mol. Cell
476 *3*, 495-504.
477 Guthold, M., Zhu, X., Rivetti, C., Yang, G., Thomson, N.H., Kasas, S., Hansma, H.G., Smith, B.,
478 Hansma, P.K. & Bustamante, C. (1999). Direct observation of one-dimensional diffusion and

479 transcription by Escherichia coli RNA polymerase. Biophys. J. *77*, 2284-2294.
480 Hampsey M., Singh, B.N., Ansari, A., Laine, J.P. & Krishnamurthy, S. (2010). Control of eukaryotic
481 gene expression: gene loops and transcriptional memory. Adv. Enzyme Regul. *51*, 118-125.
482 Harden, T.T., Wells, C.D., Friedman, L.J., Landick, R., Hochschild, A., Kondev, J. & Gelles, J.
483 (2016). Bacterial RNA polymerase can retain σ^{70} throughout transcription. Proc. Natl. Acad.
484 Sci. USA *113*, 602-607.
485 Hwang, H., Kim, H. & Myong, S. (2011). Protein induced fluorescence enhancement as a single
486 molecule assay with short distance sensitivity. Proc. Natl. Acad. Sci. USA *108*, 7414-7418.
487 Kaderi, B.E., Medler, S., Raghunayakula, S. & Ansari, A. (2009). Gene looping is conferred by
488 activator-dependent interaction of transcription initiation and termination machineries. J.
489 Biol. Chem. *284*, 25015–25025.
490 Kapanidis, A.N., Margeat, E., Laurence T. A., Doose S., Ho, S. O., Mukhopadhyay, J., Kortkhonjia,
491 E., Mekler, V., Ebright, R.H. & Weiss, S. (2005). Retention of transcription initiation factor σ^{70}
492 in transcription elongation: single-molecule analysis. Mol. Cell *20*, 347-356.
493 Larson, M.H., Greenleaf, W.J., Landick, R. & Block, S.M. (2008). Applied force reveals
494 mechanistic and energetic details of transcription termination. Cell *132*, 971-982.
495 Lee, J.Y., Finkelstein, I.J., Arciszewska, L.K., Sherratt, D.J. & Greene, E.C. (2014). Single-molecule
496 imaging of FtsK translocation reveals mechanistic features of protein-protein collisions on
497 DNA. Mol. Cell *54*, 832-843.
498 Meyer, S., & Beslon, G. (2014). Torsion-mediated interaction between adjacent genes. PLoS
499 Comput. Biol. *10*, e1003785.
500 Pannier, L., Merino, E., Marchal, K. & Collado-Vides, J. (2017). Effect of genomic distance on
501 coexpression of coregulated genes in E. coli. PLoS One *12*, e0174887
502 Ricchetti, M., Metzger, W. & Heumann, H. (1988). One-dimensional diffusion of Escherichia coli
503 DNA-dependent RNA polymerase: a mechanism to facilitate promoter location. Proc. Natl.
504 Acad. Sci. USA *85*, 4610-4614.
505 Ray-Soni, A., Mooney, R.A. & Landick, R. (2017). Trigger loop dynamics can explain stimulation
506 of intrinsic termination by bacterial RNA polymerase without terminator hairpin contact.
507 Proc. Natl. Acad. Sci. USA *114*, E9233-E9242.
508 Rocha, E.P.C. (2008). The organization of the bacterial genome. Annu. Rev. Genet. *42*, 211–233
509 Singer, P. & Wu, C.W. (1987). Promoter search by Escherichia coli RNA polymerase on a circular
510 DNA template. J. Biol. Chem. *262*, 14178-14189.
511 So, L., Ghosh, A., Zong, C., Sepulveda, L.A., Segev, R. & Golding, I. (2011). General properties of
512 transcriptional time series in Escherichia coli. Nat. Genet. *43*, 554-560.
513 Uhm, H., Kang, W., Ha, K.S., Kang, C. & Hohng, S. (2018). Single-molecule FRET studies on the
514 cotranscriptional folding of a thiamine pyrophosphate riboswitch. Proc. Natl. Acad. Sci. USA
515 *115*, 331-336.

516 Wang, F., Redding, S., Finkelstein, I.J., Forman, J., Reichman, D.R. & Greene, E.C. (2013). The
517 promoter-search mechanism of Escherichia coli RNA polymerase is dominated by three-
518 dimensional diffusion. Nat. Struct. Mol. Biol. *20*, 174-181.

519 **Supplementary Information**
520
521 # Transcription reinitiation by recycling RNA polymerase that diffuses on
522 # DNA after releasing terminated RNA
523
524 Wooyoung Kang[1,6], Kook Sun Ha[2,4,6], Heesoo Uhm[1,5], Kyuhyong Park[1], Ja Yil Lee[3], Sungchul
525 Hohng[1]*, Changwon Kang[2,7]*
526
527 [1] Department of Physics and Astronomy, and Institute of Applied Physics, Seoul National
528 University, Seoul 08826, Korea
529 [2] Department of Biological Sciences, Korea Advanced Institute of Science and Technology,
530 Daejeon 34141, Korea
531 [3] School of Life Sciences, Ulsan National Institute of Science and Technology, Ulsan 44919, Korea
532 [4] Present address: Department of Life Science, University of Suwon, Gyeonggi-do 18323, Korea
533 [5] Present address: Department of Physics, University of Oxford, Clarendon Laboratory, Parks
534 Road, Oxford OX1 3PU, United Kingdom
535 [6] These authors contributed equally
536 [7] Lead Contact
537 *Correspondence: ckang@kaist.ac.kr (C.K.); shohng@snu.ac.kr (S.H.)
538
539 ## Supplementary Tables
540
541 **Table S1. Termination efficiency and timing of various templates**

Sample	Termination efficiency (%)	Termination timing (s)
L+15	34 ± 4	4.3 ± 0.3
L+62	31 ± 3	4.2 ± 0.5
L+112	35 ± 4	5.5 ± 0.7 (without EcoRI E111Q), 4.9 ± 0.7 (with EcoRI E111Q)
L+212	34 ± 1	4.0 ± 0.8
L+312	36 ± 13	5.2 ± 1.3
L+512	36 ± 16	5.9 ± 1.4
L+112R		7.1 ± 1.3

542
543 **Table S2. Termination timing under various conditions in reinitiation experiments**

Condition	Termination timing (s)
Without sigma	5.9 ± 1.3
With sigma	6.2 ± 1.3
EcoRI E111Q binding	6.0 ± 2.3

544

545 **Table S3. Template DNA sequence**

Oligo name	Sequence (5’ → 3’)
UP8_template	TATCA AAAAG AGTAT TGACT TAAAG TCTAA CCTAT AGGAT ACTTA CAGCC ATCGA ACAGG CCTGC TGGTA ATCGC AGGCC TTTTT ATTTG GGGGA GAGGG AAGTC ATGAA AAAAC TAACC TTTGA AATTC GATCT CCAGG ATCCA CCACC
UP8M_template	TATCA AAAAG AGTAT TGACT TAAAG TCTAA CCTAT AGGAT ACTTA CAGCC ATGGC CTGCT GGTGA CTGAC TGACT GACTG AC
t500_template	TATCA AAAAG AGTAT TGACT TAAAG TCTAA CCTAT AGGAT ACTTA CAGCC ATCCC AAAGC CCGCC GAAAG GCGGG CTTTT CTGTT TCTGG GCGGT GAAGT CATGA AAAAA CTAAC CTTTG AAATT CGATC TCCAG GATCC ACCAC C
his_template	TATCA AAAAG AGTAT TGACT TAAAG TCTAA CCTAT AGGAT ACTTA CAGCC ATCCG AAAGC CCCCG GAAGA UGCAU CUUCC GGGGG CUUUU UUUUU TGGGC GGTGA AGTCA TGAAA AAACT AACCT TTGAA ATTCG ATCTC CAGGA TCCAC CACC
UP8_template_2	GCGAG ATTAC CATTA AGTGA ATTCG AAAAA AGCAC GCTAC CGCCC CAGGC GGTGG TGGAT CCTGG AGATC GAATT TCAAA GGTTA GTTTT TTCAT GACTT CCCTC TCCCC CAAAT AAAAA GGCCT GCGAT TACCA GCAGG CCTGT TCGAT GGCTG TAAGT ATCCT ATAGG TTAGA CTTTA AGTCA ATACT CTTTT TGATA
additional_part	pAATTC TTACA ATTTA GACCC TAATA TCACA TCAGA CACTA ATTGC CTCTG CCAAA ATTCT GTCCA CAAGC GTTTT AGTTC GCCCC AGTAA AGTTG TCAAT AACGA CCACC AAATC CGCAT GTTAC GGGAC TTCTT ATTAA TTCTT TTTTC GTGGG GAGCA GCGGA TCTTA ATGGA TGGCG CCAGG TGGTA TGGAA GC
additional_part_2	pGGGCT GAAAG TAGCG CCGGG TAAGG TACGC GCCTG GTATG GCAGG ACTAT GAAGC CAATA CAAAG GCTAC ATCCT CACTC GGGTG GACGG AAACG CAGAA TTATG GTTAC TTTTT GGATA CGTGA AACAT GTCCC ATGGT AGCCC AAAGA CTTGG GAGTC TATCA CCCCT AGGAC ACACA AGACA CCACA AGCTT AGACC
DNA_splint	TGTGA TATTA GGGTC TAAAT TGTAA GAATT GCGAG ATTAC CATTA AGTGA ATTCG AAAAA
DNA_splint_2	GCGTA CCTTA CCCGG CGCTA CTTTC AGCCC GCTTC CATAC CACCT GGCGC CATCC ATTAA
reinitiation_part_1B	pTAATA TCACA TCATT AGACA CTTAT CAAAA AGAGT ATTGA CTTAA AGTCT AACCT ATAGG ATACT TACAG CCTGC AGACA CCACA GACCA CACAC AAGAC ACCAC AGACC ACACA CAAGA CACCA CAGAC CACAC ACAAG ACACC ACAGA CCACA CACAA GACAC CACAG ACCAC ACACA AGACA CCACA AGCTT AGACC
DNA_splint_reinitiation	AGTGT CTAAT GATGT GATAT TAGCG AGATT ACCAT TAAGT GAATT CGAAA AA

546

547 **Table S4. Primer sequence**

Oligo name	Sequence (5’ → 3’)
forward_primer_biotin	Biotin-TATCA AAAAG AGTAT TGACT TAAAG TC
reverse_primer_biotin	Biotin-GCGAG ATTAC CATTA AGTGA A
forward_primer_Cy5	Cy5-TATCA AAAAG AGTAT TGACT TAAAG TC
reverse_primer_L+15	Cy5-CTTCC CTCTC CCCCA AATAA AAAG
reverse_primer_L+15M	Cy5-GTCAG TCAGT CAGTC AGTCA CCAGC AG
reverse_primer_L+62	Cy5-GGTGG TGGAT CCTGG AGATC G
reverse_primer_L+112	Cy5-GCGAG ATTAC CATTA AGTGA A
reverse_primer_L+212	Cy5-GACAA CTTTA CTGGG GCGAA CTAAA AC
reverse_primer_L+312	Cy5-GCTTC CATAC CACCT GGCGC CATCC AT
reverse_primer_L+512	Cy5-GGTCT AAGCT TGTGG TGTCT TGTGT GT
lambda_forward_primer	GTTTT CTGGG TTGGT

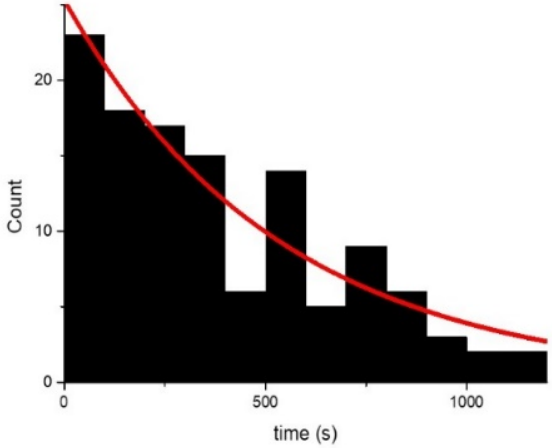

lambda_reverse_primer	GGCGG GTTTT GTTTT
forward_primer_extension	ACTAT CTATT CTCCC ATCTA TCAAA AAGAG TATTG ACTTA AAGTC
forward_primer_biotin_α	Biotin-ACTAT CTATT CTCCC ATC

Supplementary Figures

Fig. S1. RNAP·DNA complex duration at the DNA end after RNA release. We measured Cy5 PIFE survival time after the RNA release, and the distribution was fitted to a single exponential function to obtain the RNAP's retention time of 536±83 s.

557

558 **Fig. S2. Cy5 photobleaching time.**
559 To measure Cy5 survival time, we
560 performed single-molecule
561 imaging without NTP injection.
562 About 60% of the molecules
563 survived for longer than 1200 s
564 after single-molecule imaging
565 started, from which the
566 photobleaching time of Cy5 was
567 estimated as 2350 s.

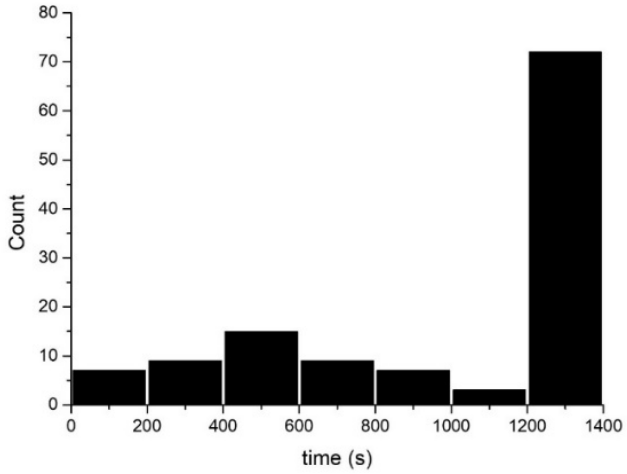

Fig. S3. Sigma retention. We estimated the percentage of transcription complex containing σ^{70} by comparing the number of Cy3-Cy5 colocalized spots between the cases of Cy5-end of DNA and those of Cy5-σ. The Cy5 labeling efficiencies of DNA (99%) and σ^{70} (105%) were similar. When Cy5 was labeled at the DNA end, 46±10% of Cy3 signal was colocalized with Cy5. When Cy5 was labeled on σ^{70}, 35±6% of Cy3 signal was colocalized with Cy5. In the figures, the green circles, red dots, and black dots indicate all Cy3 spots identified, Cy3 spots colocalized with Cy5 signal, and the Cy3 spots non-colocalized with Cy5 signal, respectively. From these results, we estimated that 75% (34.5/45.8) of elongation complex has σ^{70}.

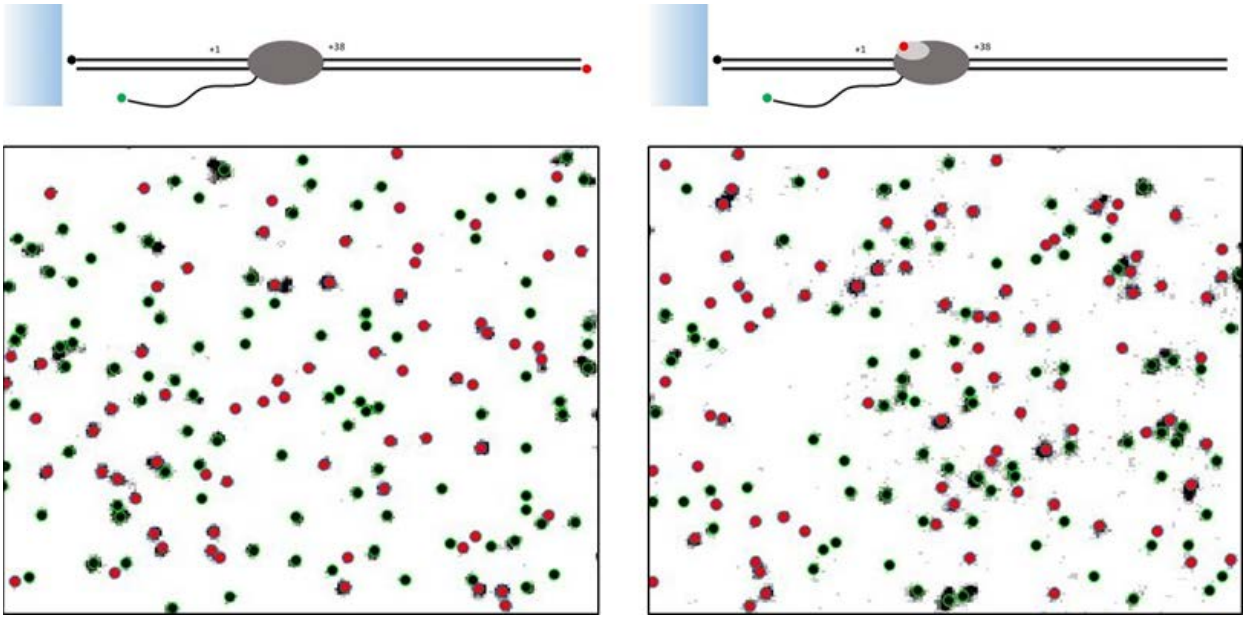

Fig. S4. σ factor lasting time at the DNA end after RNA release. We measured Cy5 signal vanishing time after NTP addition in termination complexes of Fig. 1F template.

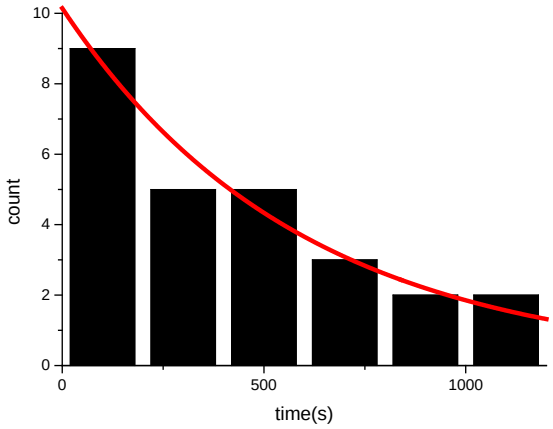

Fig. S5. E111Q inhibits the cleavage of DNA by EcoRI. Using the L+112 DNA template labeled with Cy5, we measured the cleavage inhibition efficiency of 1 nM E111Q. We counted the number of Cy5 spots before (left) and at 10 min after wild-type EcoRI injection (right) without (top) and with E111Q incubation for 5 min (bottom) before starting the imaging. The number of spots was decreased by 86±2% without E111Q incubation. On the other hand, the number was decreased by 26±4% with E111Q incubation. From these data, we estimated the cleavage inhibition efficiency of E111Q as 71±5%.

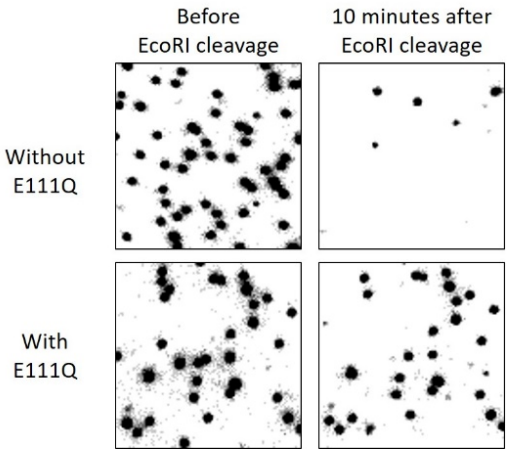

Fig. S6. Diffusion time of RNAP on a long DNA template. We prepared a transcription complex with Cy5-labled σ^{70} on a 1560-bp DNA template (L+lambda), and measured the Cy5 signal vanishing time after termination.

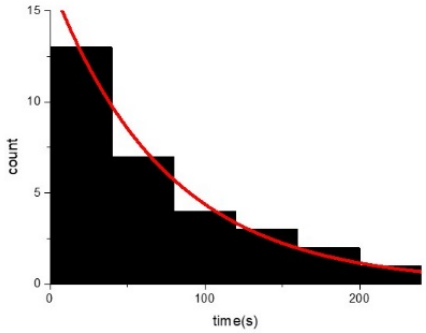
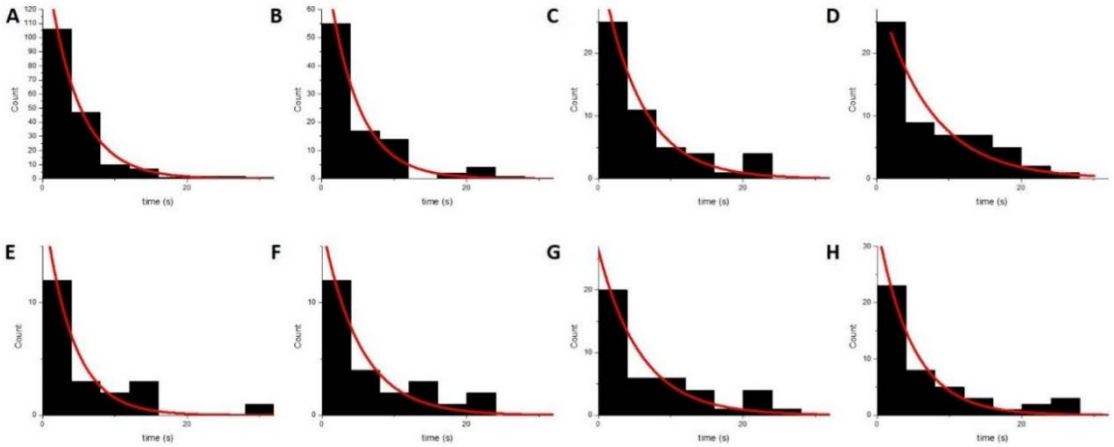
Fig. S7. Termination time of various templates. We measured the Cy3 signal vanishing time after NTP addition for L+15 (A), L+62 (B), L+112 (C), L+112R (D), L+212 (E), L+312 (F), L+512 (G) and L+112 (H) with E111Q. The distributions were fitted to a single-exponential decay function, and the fitted decay times are summarized on table S1.